# A Trajectory Optimization Strategy for Merging Maneuvers of Autonomous Vehicles

Francesco Laneve[1,2(✉)], Alessandro Rucco[2], and Massimo Bertozzi[1]

[1] Dipartimento di Ingegneria e Architettura, University of Parma, Parma, Italy
{francesco.laneve,massimo.bertozzi}@unipr.it
[2] VisLab srl, an Ambarella Company, Parma, Italy
arucco@ambarella.com

**Abstract.** In this paper we address the merging problem for Autonomous Vehicles (AVs) in presence of moving obstacles. The AV is required to follow a given desired path with a nominal (path-dependent) velocity profile, while keeping a desired safe distance with respect to moving obstacles. By using a new set of coordinates and a Virtual Target Vehicle (VTV) perspective, we propose a trajectory generation strategy to compute the (local) optimal collision-free trajectory that best approximates the desired one. In the proposed strategy, we exploit the extra degree of freedom of the VTV in order to generate a time parametrized reference, which helps to find the right space-time gap to perform a safe merging maneuver. We show the efficacy of the proposed strategy through a set of numerical computations and highlighting the main features of the generated trajectories.

**Keywords:** Autonomous vehicles · Trajectory optimization · Nonlinear optimal control

## 1 Introduction

In the last years, Autonomous Vehicles (AVs) started to run on public roads and a growing number of transport companies have started to give fully driverless rides to a limited group of people and at limited hours. This progress has led to scenarios where the interaction between the AV and human-driven vehicles must be carefully taken into account. For example, when approaching a busy intersection, the AV needs to sense the surrounding vehicles, predict their future intentions, and find the right space-time gap in order to pass before, after, or among other vehicles. Such a space-time requirement makes the analysis and design of the planning strategies particularly challenging.

Many approaches have been proposed in the literature to address this problem on different road layouts. Starting from the lane change along straight lanes, [1], different environment complexity can be taken into the problem formulation as the intersection with turning maneuvers, [2], merging into a roundabout [3]. However, all these approaches exploit inter-vehicle communications. In order to deal with the partially or fully disconnected scenarios, in [4], the authors propose a Model Predictive Control (MPC) scheme for the merging problem in a specific motorway scenario. The longitudinal motion of the merging vehicle is optimized in order to generate smooth acceleration/deceleration profiles, while the motion of the main lane vehicle (i.e., the obstacle


L. Brito Palma et al. (Eds.): CONTROLO 2022, LNEE 930, pp. 3–14, 2022.
https://doi.org/10.1007/978-3-031-10047-5_1

from the merging vehicle perspective) is used to build a penalty function for collision avoidance. Recently, the coordination of (fixed-order crossing) AVs at intersections was investigated in [5]. The proposed algorithm, based on a suitable formulation of a constrained optimal control problem, handles nonlinear dynamics, economic objective functions, and scenarios with turning vehicles. The fixed-order crossing and the collision avoidance are taken into account by introducing conflict zones and ensuring that each vehicle can occupy each conflict zone in a mutually exclusive fashion. The inter-vehicles communication assumption can be relaxed by modeling non-cooperative agents as uncertain systems and by adding suitable constraints into the optimization problem, as described in previous works of the same authors, [6] and [7].

In this paper, the merging problem is addressed from a different perspective. We assume there is no inter-vehicle communication, and we focus on the trajectory generation of the AV: we propose an optimization-based strategy in order to compute collision-free merging trajectories with the right trade-off between trajectory-tracking and maneuver-regulation behaviors (see [8–10] for a discussion on these two approaches). Specifically, given the nominal road geometry, the vehicle kinematics is initially described in terms of longitudinal and lateral coordinates. Then, based on the idea detailed in [11], we introduce the use of a Virtual Target Vehicle (VTV) that is constrained to move along the lane into which the ego vehicle have to merge. Finally, we set up a constrained optimal control problem in terms of the longitudinal and lateral coordinates and the kinematic position error between the ego vehicle and the VTV. Moreover, based on the obstacles' predictions, we enforce suitable kinematic coordinates constraints to generate collision-free trajectories. We highlight that in [11], the weighting term associated with the VTV's velocity can be used to "morph" between trajectory-tracking and maneuver-regulation features. In contrast to the previous approach, in this paper, we embed such a morphing feature into the optimization process by proposing a suitable cost function.

The rest of the paper is organized as follows. In Sect. 2, we describe the merging problem, the car model, and introduce the VTV approach. In Sect. 3, we formulate the optimal control problem. In Sect. 4, we provide numerical computations highlighting some interesting features captured by the proposed strategy.

## 2 Problem Formulation

In this section, we introduce the merging scenario, briefly describe the car model, and define a new set of coordinates.

### 2.1 The Motivating Scenario

Let us consider the merging scenario represented in Fig. 1. The intersection is composed of two incoming lanes, called the "ego lane" and the "target lane", and a crossing zone, i.e., the merging zone.

The ego vehicle is traveling along the ego lane and is supposed to merge into the target lane while performing a right turn. Moreover, the ego vehicle must yield the right-of-way to (human-driven) vehicles traveling along the target lane. From now on, we call "obstacles" the (human-driven) vehicles.

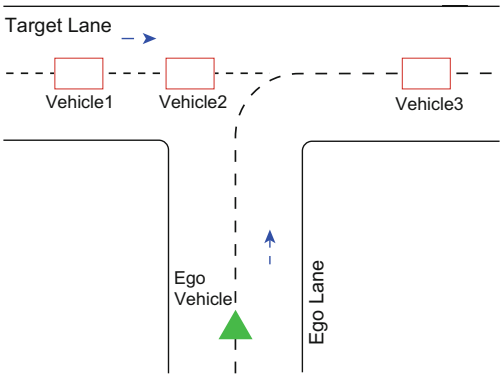


**Fig. 1.** The merging scenario. The ego vehicle is approaching an intersection where it has to yield the right-of-way to the obstacles. Travel directions are indicated by blue arrows.

We assume that i) the obstacles do not cooperate so that the ego vehicle has to find the right space-time gap to cross safely the intersection without cutting off any obstacles, and ii) the actual state (position and velocity) and the future positions of the obstacles are given (such information is usually provided by a motion forecasting module). In such a scenario, we are interested in generating a feasible trajectory for the ego vehicle that best approximates a desired one with road boundary, collision avoidance, and input control constraints. It is worth noting that, in a typical hierarchical motion planner framework, the generated trajectory can be used as a reference trajectory for a low-level controller.

### 2.2 Constrained Ego-Vehicle Model

For the sake of presentation, we focus on the case of vehicles moving on a planar road. The equations of motion are based on the well-known kinematic bicycle model and are given by

$$\begin{aligned} \dot{x} &= v\cos\psi \\ \dot{y} &= v\sin\psi \\ \dot{\psi} &= v\kappa \\ \dot{\kappa} &= u_\kappa \\ \dot{v} &= a \end{aligned} \tag{1}$$

where $(x, y)$ are the longitudinal and lateral coordinates with respect to the inertial frame, $\psi$ is the heading angle, $v$ is the velocity, and $\kappa$ is the curvature. The control inputs are the acceleration $a$ and the curvature rate $u_\kappa$. It is worth noting that we consider such a simple vehicle model for the following reasons. First, this model has no parameters, thus allowing to focus on the trajectory generation approach. Second, for urban autonomous driving, the kinematic bicycle model has comparable accuracy with a dynamic one, [12], especially for low acceleration values. For such reasons, we impose

state and input constraints on (1). In particular, the velocity is bounded by two constants $v_{min}$, $v_{max}$, i.e.,

$$v_{min} \leq v \leq v_{max} \,. \tag{2}$$

The curvature and its rate are bounded in module as follows,

$$|\kappa| \leq \kappa_{max} \,, \quad |u_\kappa| \leq u_{\kappa_{max}} \tag{3}$$

Finally, in order to take into account the passenger comfort, the longitudinal acceleration $a$ and the lateral acceleration, $v^2\kappa$, are coupled by the ellipse constraint, [2],

$$\left(\frac{a - (a_{max} + a_{min})/2}{(a_{max} - a_{min})/2}\right)^2 + \left(\frac{v^2\kappa}{a_{lat_{max}}}\right)^2 \leq 1 \,. \tag{4}$$

### 2.3 Longitudinal and Transverse Coordinates and Virtual Target Vehicle

Given a geometric path for the ego lane, we define a new set of coordinates based on the longitudinal and lateral coordinates $(s_{el}, w)$, see Fig. 2. The longitudinal coordinate $s_{el}$ represents the position along the center-line of the ego lane, whereas the lateral coordinate $w$ denotes the displacement transverse to the center-line. We assume that the ego lane has a reasonably smooth (at least $C^2$) arc-length parametrized center-line, $(\bar{x}_{el}(s_{el}), \bar{y}_{el}(s_{el}))$. The course heading $\bar{\psi}_{el}(s_{el})$ and the curvature $\bar{\kappa}_{el}(s_{el})$ are related by differentiation:

$$\begin{aligned} \frac{d\bar{x}_{el}(s_{el})}{ds_{el}} &= \cos\bar{\psi}_{el}(s_{el}) \,, \\ \frac{d\bar{y}_{el}(s_{el})}{ds_{el}} &= \sin\bar{\psi}_{el}(s_{el}) \,, \\ \frac{d\bar{\psi}_{el}(s_{el})}{ds_{el}} &= \bar{\kappa}_{el}(s_{el}) \,. \end{aligned} \tag{5}$$

Using the arc-length parametrization, the coordinates of the ego vehicle can be defined as follows:

$$\begin{bmatrix} x \\ y \end{bmatrix} = \begin{bmatrix} \bar{x}_{el}(s_{el}) \\ \bar{y}_{el}(s_{el}) \end{bmatrix} + R_z(\bar{\psi}_{el}(s_{el})) \begin{bmatrix} 0 \\ w \end{bmatrix} , \tag{6}$$

where

$$R_z(\bar{\psi}_{el}(s_{el})) = \begin{bmatrix} \cos\bar{\psi}_{el}(s_{el}) & -\sin\bar{\psi}_{el}(s_{el}) \\ \sin\bar{\psi}_{el}(s_{el}) & \cos\bar{\psi}_{el}(s_{el}) \end{bmatrix}$$

is the rotation matrix transforming vectors from the velocity frame into the inertial frame.

Next, we describe the ego vehicle position with respect to the $(s_{el}, w)$ coordinates. Following the calculations in [13], we differentiate (6) with respect to time and, by using Eqs. (1) and (5), we have

$$\begin{aligned} \dot{s}_{el} &= \frac{v\cos\mu}{1 - w\bar{\kappa}_{el}(s_{el})} \,, \\ \dot{w} &= v\sin\mu \,, \\ \dot{\mu} &= v\kappa - \bar{\kappa}_{el}(s_{el})\dot{s}_{el} \,, \end{aligned} \tag{7}$$

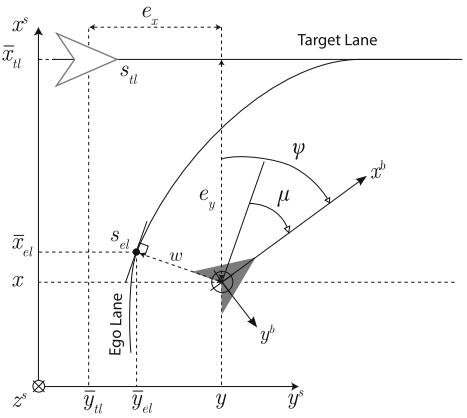


**Fig. 2.** Local coordinates around the ego and target path. The bold triangle and the empty triangle indicate the ego vehicle and the VTV, respectively. The solid lines indicate the center-line of the ego and target lane.

where $\mu = \psi - \bar{\psi}_{el}$ is the local heading error. It is worth noting that the inverse of the map $(s_{el}, w) \mapsto (x, y)$ is well-defined when the ego vehicle position is inside a tube around the center-line of the ego lane, i.e., for $1 - w\bar{\kappa}_{el}(s_{el}) > 0$.

We now introduce the VTV that should be tracked by the ego vehicle when approaching the target lane. By assuming that also the target lane has a smooth arc-length parametrized center-line, $(\bar{x}_{tl}(s_{tl}), \bar{y}_{tl}(s_{tl}))$, we constrain the VTV to move along the center-line of the target lane, see Fig. 2, so that the VTV's position can be described by simply integrating its velocity $v_{vtv}$, i.e., $\dot{s}_{tl} = v_{vtv}$. For the sake of presentation, we restrict our attention to the case of straight target lane, as the one depicted in Fig. 1.

Given the VTV's position along the target lane, $s_{tl}$, we can now describe the ego vehicle position as follows,

$$\begin{bmatrix} x \\ y \end{bmatrix} = \begin{bmatrix} \bar{x}_{tl}(s_{tl}) \\ \bar{y}_{tl}(s_{tl}) \end{bmatrix} + R_z(\psi_{tl}) \begin{bmatrix} e_x \\ e_y \end{bmatrix}, \tag{8}$$

where $e_x$ and $e_y$ are the longitudinal and lateral error coordinates, respectively, and $R_z(\psi_{tl})$ is the rotation matrix transforming vectors from the error frame into the inertial frame. Now, we differentiate (8) with respect to the time $t$ and by using the kinematic of the ego vehicle (1) we get the expression of $\dot{e}_x$ and $\dot{e}_y$ as

$$\begin{aligned} \dot{e}_x &= v \cos e_\psi - v_{vtv}\,, \\ \dot{e}_y &= v \sin e_\psi\,, \end{aligned}$$

where $e_\psi = \psi - \bar{\psi}_{tl}$ is the heading error. Finally, we re-write the nonlinear system (1) with respect to the new sets of coordinates as follows,

$$\begin{aligned}
\dot{s}_{el} &= \frac{v\cos\mu}{1 - w\bar{\kappa}_{el}(s_{el})} \\
\dot{w} &= v\sin\mu \\
\dot{\mu} &= v\kappa - \bar{\kappa}_{el}(s_{el})\dot{s}_{el} \\
\dot{\kappa} &= u_\kappa \\
\dot{v} &= a \\
\dot{s}_{tl} &= v_{vtv} \\
\dot{e}_x &= v\cos e_\psi - v_{vtv} \\
\dot{e}_y &= v\sin e_\psi
\end{aligned} \tag{9}$$

where $\mathbf{x} = [s_{el}, w, \mu, \kappa, v, s_{tl}, e_x, e_y]$ and $\mathbf{u} = [u_\kappa, a, v_{vtv}]$ are the state and control vectors.

## 3 Optimal Control Problem Formulation

In order to formulate the optimal control problem, in this section we specify additional state-input constraints and define the cost function to be optimized. We start defining two additional constraints.

First, the ego vehicle is required to satisfy the road boundaries. With respect to the new set of coordinates, this constraint assumes a very simple form: the lateral displacement $w$ is bounded in module as follows,

$$|w| \leq w_{max}\,. \tag{10}$$

Second, to generate a collision-free trajectory, we impose that, at any time $t$, the ego vehicle must be at a distance greater than $d_{collision}$ from any obstacles. Such a distance takes into account the safety distance between the ego vehicle and the obstacles, and an additional distance to model the right-of-way of obstacles (as required in the merging problem, Sect. 2.1). This constraint can be formulated by defining a circle centered at the obstacle front axes, with radius $d_{collision}$. Specifically, given the front axis position of the $i$-th obstacle and its future predictions, $(x^i_{obs}(t), y^i_{obs}(t))$, we impose that the constraint[1]

$$(x(t) - x^i_{obs}(t))^2 + (y(t) - y^i_{obs}(t))^2 \geq d^2_{collision}\,, \tag{11}$$

is satisfied for all times $t$. In order to include this constraint in the new proposed formulation, we re-write (11) with respect to the new set of coordinates obtaining the following equivalent form:

$$(s_{el}(t) - s^i_{obs}(t))^2 + (w - w^i_{obs})^2 \geq d^2_{collision}\,. \tag{12}$$

[1] For sake of presentation, we consider only circular boundary shapes, although other shapes can be taken into account.

Now we are ready to define the cost function. We start giving an informal idea of the proposed strategy, which is based on the following two observations. First, when the ego vehicle is far away from the merging zone, we are interested to follow a desired path (i.e., the center-line of the ego lane) with a desired velocity assigned to it (i.e., a space-varying velocity). Such a behavior can be captured by minimizing the following cost,

$$J_{el}(\mathbf{x}(t)) = q_1 w^2 + q_2 \mu^2 + q_3 \kappa^2 + q_4 (v - v^d(s_{el}))^2$$

where $q_1, q_2, q_3, q_4 \geq 0$.

Second, when the ego vehicle is approaching the merging zone, we are interested to track a time parameterized path (i.e., the center-line of the target lane) defined by a desired velocity $v^d(s_{tl})$. Here, we employ a quadratic cost term with respect to the kinematic position error between the ego vehicle and the VTV, and the velocity of the VTV with respect to the desired one

$$J_{tl}(\mathbf{x}(t), \mathbf{u}(t)) = q_5 e_x^2 + q_6 e_y^2 + r_1 (v_{vtv} - v_{vtv}^d(s_{tl}))^2$$

where $q_5, q_6 \geq 0$, and $r_1 > 0$.

We define the cost function as a convex combination of the previous function terms and an additional quadratic term in order to take into account the control effort:

$$J(\mathbf{x}(t), \mathbf{u}(t)) = (1 - \alpha) J_{el}(\mathbf{x}(t)) + \alpha J_{tl}(\mathbf{x}(t)) + r_2 u_k^2 + r_3 a^2 \,, \tag{13}$$

where $\alpha \in [0, 1]$ is a switch cost function based on the distance between the ego vehicle and the VTV. In particular, we use a sigmoid function $\alpha(e_x, e_y) = \frac{1}{1+\exp\left(\sqrt{e_x^2+e_y^2}-\gamma\right)}$, where $\gamma$ is a given parameter that specifies the distance from the merging zone.

We are ready to formulate the optimal control problem as follows

$$\begin{aligned} \min_{\mathbf{x}(\cdot),\mathbf{u}(\cdot)} & \int_0^{t_f} J(\mathbf{x}(\tau), \mathbf{u}(\tau))\, d\tau + m(\mathbf{x}(t_f)) \\ \text{s.t.} \quad & \dot{\mathbf{x}}(t) = f(\mathbf{x}(t), \mathbf{u}(t))\,, \ \mathbf{x}(0) = \mathbf{x}_0 \\ & h(\mathbf{x}(t), \mathbf{u}(t)) \leq 0 \end{aligned} \tag{14}$$

where $t_f > 0$ is fixed, $\dot{\mathbf{x}}(t) = f(\mathbf{x}(t), \mathbf{u}(t))$ describes the nonlinear equations (9), $h(\mathbf{x}(t), \mathbf{u}(t))$ are the state/input constraints (2), (3), (4), (10), (12) and $m(\mathbf{x}(t_f))$ is the Mayer term (a quadratic cost term). We highlight that the obstacle avoidance collision constraint (12) makes the optimization problem nonconvex and computationally challenging. In particular, we solve (14) by using the ACADO toolkit, [14]. The multiple-shooting discretization is employed with a Runge-Kutta integrator of order 4 and a sampling time of 0.2 s. The underlying Quadratic Programs (QP) are condensed and solved using an online active set strategy implemented in the software qpOASES, [15].

## 4 Numerical Computations

In this section we provide numerical computations showing the effectiveness of the proposed approach. We start with a relatively simple scenario: the ego vehicle is traveling

along the ego lane and is approaching the target lane, where an obstacle is moving. Then, as a more challenging scenario, we increase the number of obstacles. The ego lane is modeled as a $90^\circ$ right turn with a radius of 20 m. The space-varying desired velocity is equal to 7.2 m/s along the two straight sections and 5.2 m/s along the turn. The desired VTV velocity is constant along the entire target lane and equal to 7.2 m/s. The constraints parameters are based on [12] and on driving experience: $v_{min} = 0\,\mathrm{m/s}$, $v_{max} = 10\,\mathrm{m/s}$, $a_{min} = -1.5\,\mathrm{m/s^2}$, $a_{max} = 1\,\mathrm{m/s^2}$, $a_{lat_{max}} = 2\,\mathrm{m/s^2}$, $\kappa_{max} = 0.2\,\mathrm{m^{-1}}$, $w_{max} = 1.5\,\mathrm{m}$ and $d_{collision} = 10\,\mathrm{m}$. We use a planning horizon of 20 s which allows the ego vehicle to perform a merging maneuver for the entire set of numerical computations. We encourage the reader to refer to the video attachment related to the 2D plane trajectories of the numerical computations presented below, [16].

### 4.1 Merging with One Obstacle

The ego vehicle initial position is $(x_0, y_0) = (0, 0)$, with heading $\psi_0 = 0$, and velocity $v_0 = 26\,\mathrm{km/h}$ (i.e., almost $7.2\,\mathrm{m/s}$). The obstacle is in position $(x^{obs}(0), y^{obs}(0) = (35, -10)$ and is traveling along the target lane with a constant velocity of $v^{obs} = 10\,\mathrm{km/h}\,(2.78\,\mathrm{m/s})$. We solve the optimization problem (14) by setting the following weighting cost terms (obtained after a trial and error process combined with our experience in the nonlinear system (9)): $q_1 = 5.0$, $q_2 = 0.1$, $q_3 = 0.5$, $q_4 = 10.0$, $q_5 = 0.01$, $q_6 = 0.01$, $r_1 = 0.01$, $r_2 = 1.0$, and $r_3 = 0.1$. The optimal trajectory is shown in Fig. 3. Next, we analyze some interesting features of the generated trajectory. At first glance, we can identify a "pass after" behavior. Basically, the ego vehicle decelerates, thus giving the way to the obstacle (see Fig. 3f). In the generated optimal trajectory, we can identify three phases. First, at the beginning, the ego vehicle is far away from the merging area and the cost $J_{el}$ is minimized: the ego vehicle is following the center-line (the lateral displacement is almost zero), and decreases its velocity to face the right turn. Second, at about $t = 5$ s, the ego vehicle is close to the VTV and the cost $J_{tl}$ is minimized: the ego vehicle applies a positive curvature and moves toward the outside edge of the right-turn to minimize the kinematic error with respect to the VTV. Moreover, a stronger deceleration is applied (satisfying the ellipse constraint, see Fig. 3e), thus giving the way to the obstacle. Finally, we analyze the (local) optimal VTV velocity profile, see Fig. 3d. In the beginning, the VTV has zero velocity, which means that the VTV is "waiting" the ego vehicle while is traveling along the ego lane. As the ego vehicle approaches the target lane, the VTV accelerates and its velocity reaches the value of $2.78\,\mathrm{m/s}$, which is exactly the velocity of the obstacle. Consequently, the ego vehicle "tracks" the VTV position, because the $J_{tl}$ is minimized.

It is interesting to investigate how the initial obstacle position affects the generated trajectory. We set $(x^{obs}(0), y^{obs}(0) = (35, -15)$ and solve the optimization problem. The optimal trajectory is shown in Fig. 4. In the beginning, the ego vehicle follows the ego lane path with the desired velocity. When approaching the target lane, the optimizer finds enough time-space gap to perform a "pass before" the obstacle. The VTV velocity increases with a sharp acceleration, and the ego vehicle starts to track the VTV: first, it moves toward the inside edge of the turn (the so-called apex point is almost reached) in order to minimize the curvature and satisfy the acceleration constraint and, second, it accelerates in a smooth fashion.

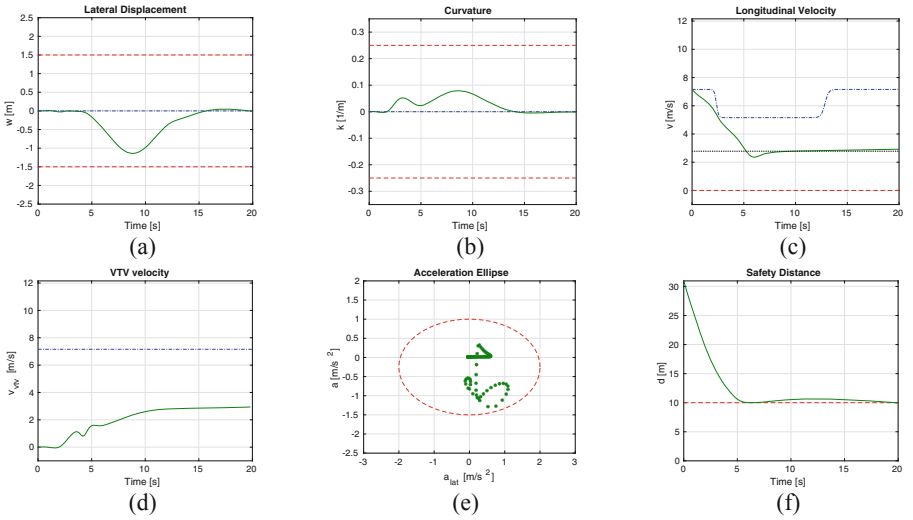


**Fig. 3.** Merging with one obstacle: pass after behavior. The optimal (green solid line), the desired (blue dash-dot line) trajectories, and constraints (red dash lines) are shown. Obstacle initial position $(x^{obs}(0), y^{obs}(0)) = (35, -10)$.

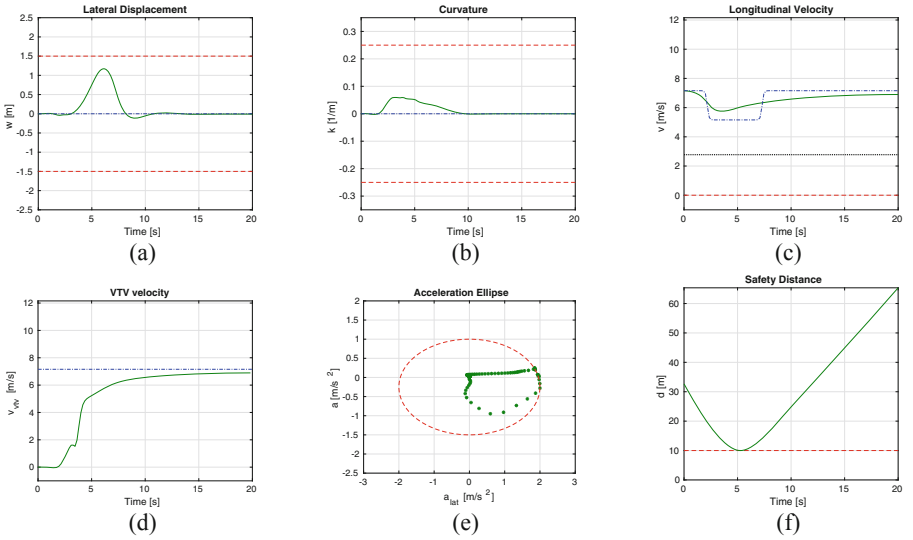


**Fig. 4.** Merging with one obstacle: pass before behavior. The optimal (green solid line), the desired (blue dash-dot line) trajectories, and constraints (red dash line) are shown. Obstacle initial position $(x^{obs}(0), y^{obs}(0)) = (35, -15)$.

### 4.2 Merging into Traffic

We consider four obstacles traveling along the target lane to simulate a more challenging scenario. The obstacles are located at $(x_1^{obs}(0), y_1^{obs}(0)) = (35, 5)$, $(x_2^{obs}(0), y_2^{obs}(0)) = (35, -13)$, $(x_3^{obs}(0), y_3^{obs}(0)) = (35, -29)$ and $(x_4^{obs}(0), y_4^{obs}(0)) = (35, -51)$ and are moving along the target lane with a velocity of 3.3 $\mathrm{m/s}$ (12 $\mathrm{km/h}$). The initial position, orientation and velocity of the ego vehicle are $(x, y) = (0, 0)$, $\psi = 0$ and $v_0 = 26$ $\mathrm{km/h}$(7.2 $\mathrm{m/s}$), respectively. The optimal trajectory is shown in Fig. 5. The ego vehicle starts the maneuver by following the ego lane reference velocity, see Fig. 5c, for $t \in [0, 2]$ s. At about 3 s, the ego vehicle is approaching the target lane, and the $J_{tl}$ is minimized. Indeed, we highlight that: i) the ego vehicle decelerates to stop before the intersection (so that the collision avoidance is always satisfied), ii) slightly moves toward the inner edge of the right turn to gain the best position for the merging, and iii) the VTV moves towards to minimize the kinematic error (mainly because the projection of the ego vehicle to the target lane corresponds to a point which is slightly moving forward). In fact, there is no space-time gap to perform a merging maneuver. Now, while the obstacle1 has already crossed the intersection zone, the vehicle has performed a full stop, thus giving the way to obstacle2 and obstacle3 (see Fig. 5f). At about $t = 10$ s, the right space-time gap is found: the VTV accelerates and the ego vehicle starts tracking the VTV position, thus performing a safe "pass before" obstacle4.

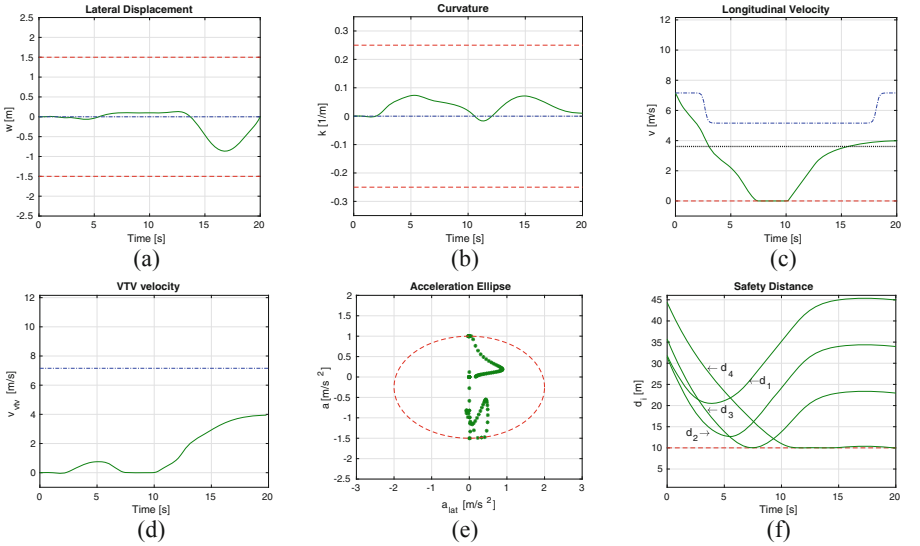


**Fig. 5.** Merging with four obstacles: Pass among behavior. The optimal (green solid line), the desired (blue dash-dot line) trajectories and constraints (red dash line) are shown.

## 5 Conclusions

In this paper we proposed a strategy for the trajectory generation of an autonomous vehicle in a merging scenario with non-cooperative obstacles. The proposed formulation takes the advantage of the use of transverse coordinates and the virtual target vehicle approach to capture interesting dynamics features. In particular, an optimization strategy based on optimal control problem has been developed to generate a feasible merging trajectory, and at the same time, guarantees collision avoidance in the presence of obstacles. We evaluated the proposed strategy in a simulated scenario and showed that the proposed approach can successfully generate a merging trajectory, allowing the AV to perform a safe merging even in presence of multiple obstacles. Future work will focus on i) the extension of the proposed strategy in order to take into account the accuracy of the obstacles' position/velocity, ii) the validation in more complex scenarios (e.g., multiple lanes).

## References

1. Hidalgo, C., Lattarulo, R., Flores, C., Pérez, R.J.: Platoon merging approach based on hybrid trajectory planning and CACC strategies. Sensors **21**(8), 2626 (2021)
2. Hult, R., Zanon, M., Gros, S., Falcone, P.: Optimal coordination of automated vehicles at intersections with turns. In: 2019 18th European Control Conference (ECC), pp. 225–230. IEEE (2019)
3. Debada, E.G., Gillet, D.: Virtual vehicle-based cooperative maneuver planning for connected automated vehicles at single-lane roundabouts. IEEE Intell. Transp. Syst. Mag. **10**(4), 35–46 (2018)
4. Cao, W., Mukai, M., Kawabe, T.: Merging trajectory generation method using real-time optimization with enhanced robustness against sensor noise. Artif. Life Robot. **24**(4), 527–533 (2019). https://doi.org/10.1007/s10015-019-00546-w
5. Hult, R., Zanon, M., Gros, S., Falcone, P.: A semidistributed interior point algorithm for optimal coordination of automated vehicles at intersections. IEEE Trans. Control Syst. Technol. (2021). https://doi.org/10.1109/TCST.2021.3132835
6. Batkovic, I., Zanon, M., Ali, M., Falcone, P.: Real-time constrained trajectory planning and vehicle control for proactive autonomous driving with road users. In: 2019 18th European Control Conference (ECC), pp. 256–262. IEEE (2019)
7. Batkovic, I., Ali, M., Falcone, P., Zanon, M.: Safe trajectory tracking in uncertain environments. arXiv preprint arXiv:2001.11602 (2020)
8. Aguiar, A.P., Hespanha, J.P.: Trajectory-tracking and path-following of underactuated autonomous vehicles with parametric modeling uncertainty. IEEE Trans. Autom. Control **52**(8), 1362–1379 (2007)
9. Aguiar, A.P., Hespanha, J.P., Kokotović, P.V.: Performance limitations in reference tracking and path following for nonlinear systems. Automatica **44**(3), 598–610 (2008)
10. Saccon, A., Hauser, J., Beghi, A.: A virtual rider for motorcycles: maneuver regulation of a multi-body vehicle model. IEEE Trans. Control Syst. Technol. **21**(2), 332–346 (2012)
11. Rucco, A., Aguiar, A.P., Hauser, J.: Trajectory optimization for constrained UAVs: a virtual target vehicle approach. In: 2015 International Conference on Unmanned Aircraft Systems (ICUAS), pp. 236–245. IEEE (2015)
12. Kong, J., Pfeiffer, M., Schildbach, G., Borrelli, F.: Kinematic and dynamic vehicle models for autonomous driving control design. In: 2015 IEEE Intelligent Vehicles Symposium (IV), pp. 1094–1099. IEEE (2015)

13. Bayer, F., Hauser, J.: Trajectory optimization for vehicles in a constrained environment. In: 2012 IEEE 51st IEEE Conference on Decision and Control (CDC), pp. 5625–5630. IEEE (2012)
14. Houska, B., Ferreau, H.J., Diehl, M.: ACADO toolkit - an open source framework for automatic control and dynamic optimization. Optim. Control Appl. Methods **32**(3), 298–312 (2011)
15. Ferreau, H.J., Kirches, C., Potschka, A., Bock, H.G., Diehl, M.: qpOASES: a parametric active-set algorithm for quadratic programming. Math. Program. Comput. **6**(4), 327–363 (2014). https://doi.org/10.1007/s12532-014-0071-1
16. Video attachment. https://youtu.be/jyvSBll2uWA